PERGAMON

Atmospheric Environment 36 (2002) 4863–4876

ATMOSPHERIC ENVIRONMENT

www.elsevier.com/locate/atmosenv

Characterization of sources and emission rates of mineral dust in Northern China

Jie Xuan, Irina N. Sokolik*

Program in Atmospheric and Oceanic Sciences, University of Colorado at Boulder, Boulder, CO 80309, USA

Received 2 January 2002; accepted 16 July 2002

Abstract

Northern China, covering many deserts, gobi-deserts and arid loess-lands, is one of the world's largest sources of atmospheric dust. In this study, we estimate the dust annual mean emission rates and perform comparative characterization of dust sources in Northern China by combining the geographical, pedological and 30-year (1951–1980) climatological data. Multi-year averaged emission rates of PM_{50}, PM_{30} and PM_{10} (i.e., dust particulates smaller than 0.05, 0.03 and 0.01 mm in diameter, respectively) were calculated using the modified US EPA empirical formulas. We demonstrate that the main dust sources in Northern China are the Taklimakan Desert (the annual mean PM_{10} emission rate, Q_{10}, is some 0.38 ton/ha yr), the Central gobi-desert ($Q_{10} = 0.24$ ton/ha yr), and the deserts located on the Alxa Plateau ($Q_{10} = 0.05$ ton/ha yr). The Loess Plateau appears to be a weak dust source. We identify and characterize three broad types of dust sources in Northern China: Type 1. Deserts in dry-agricultural areas, Type 2. Gobi-deserts and deserts located on the plateaus, and Type 3. Deserts and gobi-deserts located in topographical lows. Types 1–3 sources contribute 1%, 35% and 64%, respectively, to the total annual mean emission of PM_{10} dust. Although the maximum of dust emission occurs in spring, each source type has a distinct seasonal cycle. The analysis of both the seasonal cycle pattern and spatial distribution of dust emission rates demonstrates that a combination of extreme aridity and strong winds is a key factor governing the dust emission in Northern China.

Keywords: Wind-blown mineral dust; Dust source region; PM_{10}; Emission rate; China

1. Introduction

Wind-blown mineral dust, once lifted into the atmosphere, causes diverse effects on health, environment and climate (Goudie and Middleton, 1992; Duce, 1995; Sokolik et al., 2001). The magnitude of the impact depends on the amount and the physical and chemical properties of atmospheric dust that are largely controlled by dust sources. Natural deserts and semi-arid lands are believed to be a main supplier of atmospheric dust. They cover approximately 33% of the world land area, having inhomogeneous geographical distribution and distinct features (Duce, 1995). In addition, various human activities can alter the geographical area of dust sources and increase dust loading into the atmosphere. Current estimates of global annual mean dust burden are poorly constrained, spanning a range from about 1000 to 5000 Tg/yr (IPCC, 2001). Uncertainties are mainly due to a poor knowledge of the strength of diverse individual sources. A better quantification of dust burden on regional scales is necessary if climate and climatic change predictions are to be improved.

This study deals with the dust sources located in Northern China (35°–54°N, 73°–135°E). Northern China is the second largest source of atmospheric dust in the world. Each year, mainly in winter and spring seasons, strong winds lift and transport a large amount of dust. The considerable fraction of dust particles can be carried out eastward for thousands of kilometers

*Corresponding author.
E-mail address: sokolik@lasp.colorado.edu (I.N. Sokolik).

1352-2310/02/$ - see front matter
PII: S1352-2310(02)00585-X

across the Pacific and beyond to the west coast of the United States, affecting the large geographical region. Understanding and predicting the overall dust impacts in this region depend critically on knowledge of dust sources and emission rates. Although a number of previous studies have addressed to various extent the characterization of dust storms in Northern China (e.g., Xu and Hu, 1996; Qian et al., 1997; Xuan, 1999), identification of active dust sources and quantification of their strengths in this region remains an unresolved issue. To address this problem, we compiled and analyzed a large data set called the Asian Dust Databank. Currently, the Databank comprises the geographical, pedological and 30 yr (1951–1980) climatological data from 301 meteorological stations in Northern China.

The goals of this paper are to identify and characterize the main dust production regions in Northern China and to quantify the strength of the sources in terms of dust emission rates on the climatic (30 yr mean) time scale. To estimate annual and seasonal mean dust emission rates, we employ the empirical formulas developed by the United States Environmental Protection Agency (EPA) (OAQPS, 1977; Cowherd et al., 1979). The EPA empirical formulas predict annual mean emission rates using measured soil and climate parameters. They seem to be appropriate in this study since we are interested in the multi-year averaged strength of the dust sources.

It has been recognized that dust mobilization is a complex process controlled by specific surface properties and local meteorological conditions. Therefore, a combination of these factors must be considered to adequately quantify the strength of a dust source. To guide the characterization of dust sources, we introduce an integrated set of the following factors: the frequency of dust storm occurrence, wind speed, aridity and precipitation, morphology and composition of surface soil, and dust emission rates. Combining these factors, we perform comprehensive, comparative characterization of dust sources in Northern China, identifying their commonalities and specific features that affect the dust mobilization. We also address the effects of human activities on dust emission in this region.

This paper is organized as follows. A methodology of dust emission calculation is described in Section 2. Then, in Section 3, we focus on comparative characterization of dust sources in Northern China followed by Summary.

2. Quantification of a source strength

2.1. Approaches in dust emission modeling

The complexity and various aspects of the dust mobilization by winds have been addressed by numerous studies (e.g., Bagnold, 1941; Greeley and Iversen, 1985; Gillette, 1979). A number of key factors controlling the dust emission have been identified and some of them have been incorporated into dust production schemes used in climate and atmospheric chemical transport models (e.g., Tegen and Fung, 1995; Marticorena and Bergametti, 1995). Despite the recent progress, those schemes rely on oversimplified assumptions resulting in large uncertainties in the prediction of dust loadings and hence adverse dust impacts (IPCC, 2001; Sokolik et al., 2001).

Dust production schemes currently used in atmospheric dynamical models are mainly based on an assumption that the vertical dust flux, F, is a power-law function of the wind friction velocity, u_* (or wind velocity, u)

$$F = C\,u_*^n, \tag{1}$$

where C is a dimensional constant. Dust production occurs when u_* is equal or larger than a threshold friction velocity, $u_{*\mathrm{tr}}$. Both C and $u_{*\mathrm{tr}}$ are a complex function of local meteorological conditions and surface properties (soil texture, mineralogy, vegetation coverage and surface roughness among other factors). Moreover, several experimental and theoretical studies demonstrated that the exponent n in Eq. (1) varies between 3 and 4, but it might be as high as 7 (Gillette, 1979).

As a practical necessity, it is often assumed that n is equal to 3 or 4, and C and the threshold friction velocity $u_{*\mathrm{tr}}$ are prescribed constants. For instance, Tegen and Fung (1995), Tegen and Miller (1997), and Uno et al. (2001) approximated the dust vertical flux by

$$F = C_1(u - u_{\mathrm{tr}})u^2, \tag{2}$$

assuming $n = 3$ and the threshold wind velocity $u_{\mathrm{tr}} = 6.5\,\mathrm{m/s}$. In turn, Westphal et al. (1998), Liu and Westphal (2001) and several others used the dust production scheme in a form

$$F = C_2 u_*^4, \tag{3}$$

where C_2 is the dimensional constant, assuming $u_{*\,\mathrm{tr}} = 0.6\,\mathrm{m/s}$.

Such an approach raises several key problems. Firstly, dust production would depend on how well an atmospheric dynamical model can predict meteorological fields and, in particular, the surface winds used in Eqs. (2) and (3). Several studies demonstrated that there are significant differences in the surface winds predicted by different models (e.g., Liu and Westphal, 2001). The advantage of the EPA formulas employed in our study is that they allow us to use the observed winds available from numerous meteorological stations in Northern China as described below.

Another problem in the dust production schemes (Eqs. (2) and (3)) is in the selection of a constant C and threshold friction velocity, $u_{*\mathrm{tr}}$. Recently, an improved

scheme has been proposed by Marticorena and Bergametti (1995), in which the threshold friction velocity is parameterized as a function of the particle size distribution, $N(d)$, of erodible soil particles and the roughness length, z_0, of the land surface. This scheme has been tested for Saharan deserts (Marticorena et al., 1997) and recently it was adopted to compute the dust emission in southwestern Asia (Iraq, Kuwait, and Saudi Arabia) during 1990–1991 (Draxler et al., 2001). However, implementation of such a scheme requires input data, which are largely missing (especially in Northern China). Because of this lack, we could not employ the above scheme in this study. One of our goals in developing the Asian Dust Databank is to provide the currently missing data so that a better dust production scheme for Northern China can be developed.

2.2. Computation of dust emission rates

We employed the Asian Dust Databank in conjunction with the EPA empirical formulas to compute annual mean dust emission rates in Northern China. EPA formulas are based on numerous measurements of dust emission from various surfaces under different meteorological conditions (OAQPS, 1977; Cowherd et al., 1979). This allows for calculation of PM_{30} and PM_{50} annual mean emission rates as

$$Q_{30} = 0.2058\, e\, s\, f/\mathrm{PE}^2, \tag{4}$$

$$Q_{50} = e\, c_{50} C\, K\, L\, V, \tag{5}$$

where Q_{30} and Q_{50} denote the annual mean dust emission rates, in units of ton/ha yr, for PM_{30} and PM_{50}, respectively, f is the threshold wind speed ratio (i.e., time percentage when the mean wind speed u is higher than a threshold value of 5.4 m/s), C is so-called climatic factor defined as $C = 0.504u^3/\mathrm{PE}^2$, where PE is the Thornthwaite's precipitation–evaporation index (see Table 1), K is the surface roughness factor, L is the unsheltered field width factor, and V is the vegetation cover factor. The soil parameters e, s, c_{50} are defined in Table 1 along with other parameters required to compute the annual mean dust emission rates using Eqs. (4) and (5). Table 1 also lists the data used in calculations.

Overall, we analyzed the data from 301 meteorological stations in Northern China for the period 1951–1980. The meteorological stations are distributed inhomogeneously: more stations are in the dense-populated areas and just a few in the northwest deserts. To provide even coverage over Northern China, the data were interpolated to 92 grid points, providing a spatial resolution of about $2.5^\circ \times 2.5^\circ$ (see Fig. 1). The limited number of stations in the northwest deserts (especially in the Taklimakan) renders the finer resolution unreasonable.

Both soil and climatic data were pre-processed to provide input parameters required in the EPA formulas. For instance, there were no data for e, s, and c_{50}. To provide the input soil data, we converted the soil type data using China's soil texture maps (Xiong and Li, 1990; Xiong, 1986) into correspondent types used in the US.

The Thornthwaite's precipitation–evaporation index, PE, required in Eqs. (4) and (5) is not commonly used by Chinese scientists. Instead, the aridity, R, is used in classification of the climatic zones. The aridity is

Table 1
Input parameters and data used in EPA formulas

Parameter	Definition (units)	Data used in calculations
Erodibility index, e	Mass loss by wind erosion (ton/ha yr)	Xiong (1986)[a]
Silt content, s	Weight percentage of soil particles smaller than 0.075 mm (%)	Xiong (1986)[a]
Soil texture parameter, c_{50}	Weight percentage of soil particles smaller than 0.050 mm (%)	Xiong (1986)[a]
Threshold wind speed, u_{tr}	Large particles start to creep at u_{tr} (m/s)	$u_{tr} = 5.4$ m/s
Annual mean wind speed, u	Annual mean wind speed at 10 m height (m/s)	301 Met. Stations, 1951–1980
Threshold wind speed ratio, f	Annual time percentage of $u > u_{tr}$	[a]
Annual mean precipitation, p	(mm/yr)	301 Met. Stations, 1951–1980
Annual mean evaporation, e_e	(mm/yr)	301 Met. Stations, 1951–1980
Thornthwaite's precipitation–evaporation index, PE	$\mathrm{PE} = 300p/e_e$[a]	Same as for p and e_e
Climatic factor, C	$C = 0.504\, u^3/PE^2$	Same as for u and PE
Surface roughness factor, K	$K = 1$ or 0.5 for smooth or rough surfaces, respectively	$K = 0.5$
Unsheltered field width factor, L	$L = 0.7$ or 1.0 for fields of width <300 m or >600 m, respectively	$L = 1.0$
Vegetation cover factor, V	$V = 1.0$ if no vegetation	$V = 1/8$

[a] See details on data pre-processing in Xuan (1999) and Xuan et al. (2000).

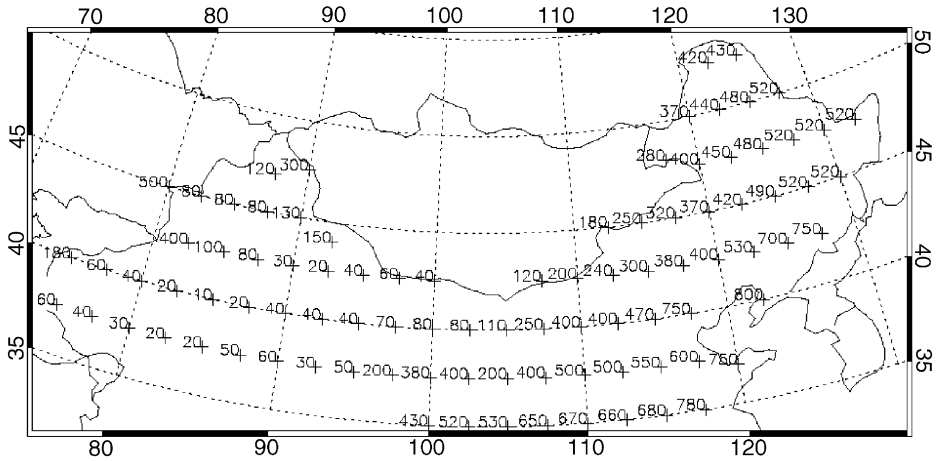

Fig. 1. Annual mean precipitation (mm/yr) at 92 grid points (crosses) used in calculations.

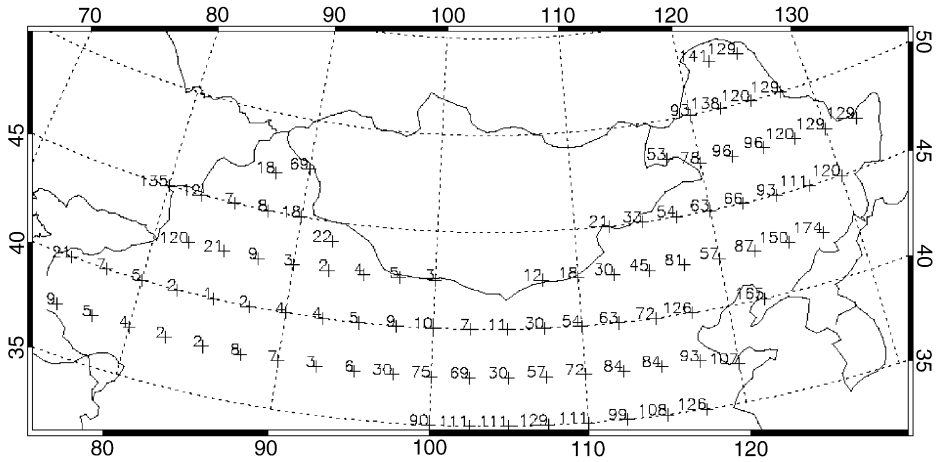

Fig. 2. Same as Fig. 1, except for Thornthwaite's precipitation–evaporation index, PE.

defined as

$$R = 0.16\,\Sigma T/p, \tag{6}$$

where ΣT is the accumulated diurnal mean air temperature higher than 10°C and p is the precipitation for the same time period (Zhao, 1985). In our study we analyze both the aridity and PE index. The latter was calculated with precipitation and evaporation data reported by the weather stations. Figs. 1–3 show 30 yr annual mean precipitation, PE and aridity, respectively, at 92 grid points used in our calculations. One can notice a strong east-to-west decrease in the precipitation and PE values and an east-to-west increase in aridity. These east-to-west gradients are particular characteristics of climate in Northern China, and play a key role in controlling the dust emission pattern as demonstrated below.

The threshold wind speed ratio, f (see Table 1), was calculated using the annual mean wind speed following Xu (1984). Fig. 4 shows 30 yr annual mean f at 92 grid points. One can notice that, on the Inner-Mongolia Plateau (refers to the Chinese part of the Mongolian Plateau), wind speed is higher than the threshold value of 5.4 m/s for about 20–40% of time per year. The study by Zhang and Lin (1992) based on the 20 yr mean data reported the spatial distribution of the number of days with gales (maximum wind speed > 17 m/s). They show that the area along the Chinese–Mongolian border has the largest number of days with gales (about 75 days a year). They also concluded that the areas with highest mean wind speeds are also those with the largest number

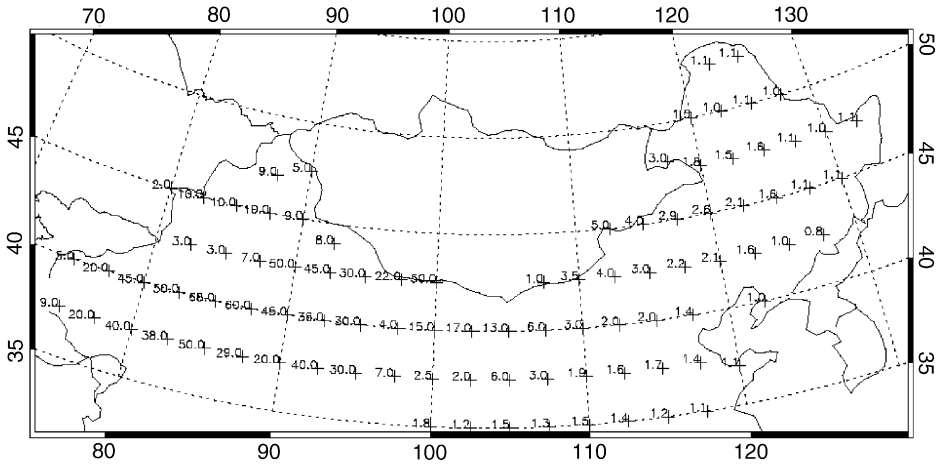

Fig. 3. Same as Fig. 1, except for annual mean aridity.

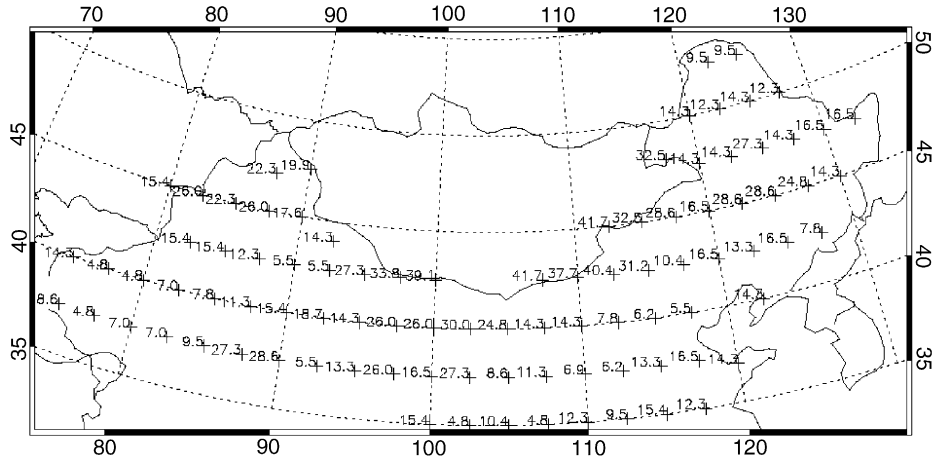

Fig. 4. Same as Fig. 1, except for the threshold wind speed ratio.

of gales. The same statement is true for the distribution of the annul mean wind speed and f, indicating that the emission rates Q_{30} and Q_{50} calculated with Eqs. (4) and (5) will show the similar pattern.

The annual mean emission rates Q_{30} and Q_{50} were first calculated at 92 grid points using Eqs. (4) and (5), then the PM_{10} annual emission rates, Q_{10}, were calculated following the procedure described below. The basic assumption of the EPA empirical formulas is that the emission rate, Q_d, of the particulates smaller than d mm in diameter is proportional to the weight percentage of those particulates in the surface soil

$$Q_d \sim c_d. \tag{7}$$

Thus, the soil texture parameter, c_{30} (i.e., the weight ratio of particles smaller than 0.03 mm in diameter over total erodible soil particles) can be calculated with c_{50} as follows:

$$k = \frac{c_{30}}{c_{50}} = \frac{Q_{30}}{Q_{50}}. \tag{8}$$

Using Q_{30} and Q_{50} computed at 92 grid points, we determine from Eq. (8).

$$k = 0.62. \tag{9}$$

The particle size distribution is commonly approximated by a lognormal function (e.g., Bagnold, 1941), so that the soil texture parameter c_d can be expressed as

$$c_d = \frac{1}{\sqrt{2\pi}\sigma} \int_{-\infty}^{y} \exp\left[-\frac{(t-\mu)^2}{2\sigma^2}\right] \mathrm{d}t, \tag{10}$$

where $y = \log(d)$, and μ and σ are two parameters of the lognormal function.

First, the soil texture parameter c_{30} was calculated using Eqs. (8) and (9) for each of the 92 grid points. Next, using calculated c_{30} and c_{50}, the parameters μ and σ were determined from Eq. (10). Letting $d = 0.01$ mm (i.e., $y = \log 0.01 = -2$) in the Eq. (10), we then obtained c_{10}. Finally, the PM_{10} annual dust emission rates, Q_{10}, were calculated as

$$Q_{10} = Q_{50}\frac{c_{10}}{c_{50}}. \quad (11)$$

Following the above procedure, we computed the emission rates Q_{50}, Q_{30}, and Q_{10}, which then were used to characterize the strength of dust sources, as well as to analyze spatial patterns and temporal variations of the annual and seasonal mean dust emission in Northern China.

3. Characterization of dust sources in Northern China

Sources of atmospheric wind-blown dust are often categorized based on one or two types of observational data. For instance, Goudie and Middleton (1992) and Sun et al. (2001) used the records of dust storm occurrences from weather stations in China. However, a small number of stations with limited spatial coverage were considered in those studies. Moreover, the dust outbreaks were not related to actual dust sources. The recent study by Prospero et al. (2002) utilized the aerosol index (AI) retrieved from the satellite total ozone mapping spectrometer (TOMS) data to identify the active dust sources. Although UV remote sensing provides a powerful tool in characterizing the large areas affected by dust, persistent clouds and air pollution (especially UV-absorbing carbonaceous aerosols) limit the application of the TOMS AI over much of Asia. In addition, complex topography of Northern China hinders the interpretation of the AI values.

Given the complexity of dust mobilization processes, we believe that the approaches based on a single characteristic would not be adequate for the comprehensive characterization of a dust source. Below we introduce an integrated set of the factors used in our study to identify and quantitatively characterize the dust sources.

3.1. The factors for identification and characterization of dust sources

We propose the following set of the factors for the analysis of dust sources: the frequency of dust storm occurrence, wind speed, aridity and precipitation, morphology and composition of surface soil, and dust emission rates.

3.1.1. Frequency of dust storm occurrence

Dust storms are often defined as an event of dust particles entrained by winds so that the meteorological visibility is decreased below 1 km (Goudie and Middleton, 1992; CMA, 1979). Based on visibility observations, dust storms have been recorded at the meteorological stations in China since 1951, while various records of dust storms are available for the past 4600 yr (Huang, 1997).

Fig. 5 shows the regions of high and extra-high frequency of dust storm occurrence based on the analysis of 30 yr (1951–1980) climatic data. To cover entire Northern China, we extended the analysis of Xu and Hu (1996), who considered only Northwest China. High frequency regions are defined as those having: (i) the annual mean number of dust storm days higher than 5; or (ii) monthly mean number higher than 3; or (iii) the total number of dust storm days at any month for 10 continuous years higher than 20. In turn, the extra-high frequency regions have: (i) the annual mean number of dust storm days higher than 12; or (ii) the total number of dust storm days at any month for 19 continuous years higher than 30.

The high-frequency regions cover all main deserts and gobi-deserts in Northern China. The only exception is the newest Hulun Buir Desert located in the east edge of

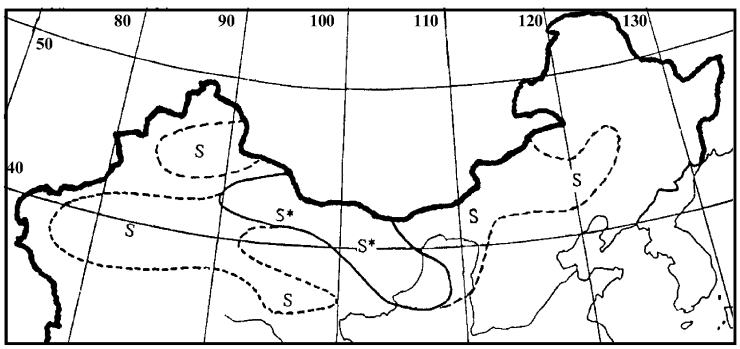

Fig. 5. Frequency of dust storm occurrence: high frequency area (*S*) and extra-high frequency area (*S**).

the Inner-Mongolia Plateau. The Loess Plateau is not included in the high-frequency regions except for its northwest borderland adjacent to the deserts. The most severe dust storms are mainly recorded in the west part of the Inner-Mongolia Plateau, Alxa Plateau and Hexi Corridor (Xu and Hu, 1996; Zhao, 1997).

There is no doubt that the high frequency of dust storms is an important indicator of the source area. However, strong dust outbreaks could be transported over large distances and reported by the weather stations located outside an actual active source. There are only a few stations located in the deserts. Therefore, the frequency of dust storm occurrence must be considered in a combination with other data.

3.1.2. Wind speed

The dust emission occurs only when the wind speed is higher than a threshold value. The greater wind speed the larger fraction of dust particles can be lifted from the surface, increasing the dust emission rates. Strong winds associated with the Arctic anticyclones are a distinct climatic feature of Northern China. The Siberian Highs (or Mongolian Highs) cause strong cold waves that funnels cold air across Mongolia and China. It is believed that major dust outbreaks are caused by those cold waves. The highest winds are commonly observed in the winter and spring, having the maximum values over the large area of the Mongolian Plateau.

3.1.3. Aridity and precipitation

Northern China is surrounded by highlands at three sides—the Mongolian Plateau to the north, the Pamir Plateau to the west and the Tibetan Plateau to the south. The elevation of the Tibetan Plateau is around 5000 m. Only in the summer season, monsoon winds from the Pacific Ocean can bring some moisture to the region. However, the precipitation is very limited and sharply decreases from east to west in Northern China (see Fig. 2). High frequency and extra-high frequency dust storm regions have precipitation $p<400$ and 200 mm/yr, respectively. Also, the high and extra-high frequency dust storm regions are characterized by the Thornthwaite's index $PE<60$ or the aridity $R>2$. In general, aridity $R=1.5-2.0$ defines the semi-arid region, $R>2.0$ is for the arid region, and $R>4.0$ is for the deserts and gobi-deserts.

One might expect that dust emission is higher in the regions with low precipitation (and consequently scarce vegetation) and high aridity. Indeed, Hao et al. (1996) analyzed the annual variation of dusty days (defined as horizontal visibility less than 10 km) in the Beijing Metropolitan Area and concluded that the number of dusty days per year is negatively correlated with the annual precipitation and vegetation cover rate. Also, Sun et al. (2001) showed that the annual number of dust storm days in Northern China is positively correlated with annual mean wind speed but negatively correlated with annual precipitation. In general, precipitation controls the atmospheric dust burden: (1) by affecting surface soil moisture, vegetation cover, and soil crust and hence the emission rate; and (2) by removing airborne dust particles via rain out.

3.1.4. Morphology and composition of surface soil

Soil texture, mineralogical composition, aggregation and crusting are main surface soil characteristics affecting the dust emission.

The soil particle size distribution (or soil texture) is important because several processes controlling the dust emission are size dependent. Particles of around 60–80 μm in diameter have a minimum threshold friction velocity (e.g., Bagnold, 1941). Thus, the abundance of loose particle in this size range is critical to initiate the mobilization. Traditionally, soil texture is classified in terms of three end members: clay ($d<0.002$ mm), silt ($0.002<d<0.05$ mm), and sand ($0.05<d<2$ mm). The Chinese classification system, which is somewhat similar to the US system, is based on four first grade categories (clay, loam, sand and gravel) and 12 second grade categories (Xiong and Li, 1990).

Another important characteristic is the soil mineralogical composition which affects the degree of aggregation of soil grains and surface crusting and hence the threshold wind velocity. Both clay aggregation and surface crust resist wind erosion. In particular, it has been demonstrated that soils with high clay content ($>20\%$) highly resistant to wind erosion (Gillette, 1979).

In addition, Northern China is characterized by a variety of surface types including farmland, grassland, desert and gobi-desert. The term 'gobi' is used to describe a region paved with gravel or rock debris and 'gobi-desert' refers to an area of alternatively distributed sandy deserts, gobis and grasslands (Chao, 1984). Gobi and gobi-deserts exist only in the extremely arid areas, such as the northern and western Inner-Mongolia Plateau and its southwest vicinity.

3.1.5. Dust emission rates

The emission rate is often used to characterize the strength of a source. Depending on a specific application, emission rates of dust particles in the different size range might be of interest. PM_{50} and PM_{30} dust plays an important role in the biogeochemical cycles of the oceans and terrestrial systems by supplying a large mass fraction of micronutrients. PM_{10} dust can scatter and absorb solar and infrared radiation affecting the Earth's energy budget and climate. In addition, PM_{10} dust also causes the degradation of visibility and various health problems. Therefore, Q_{50}, Q_{30} and Q_{10} emission rates were computed and analyzed in this study.

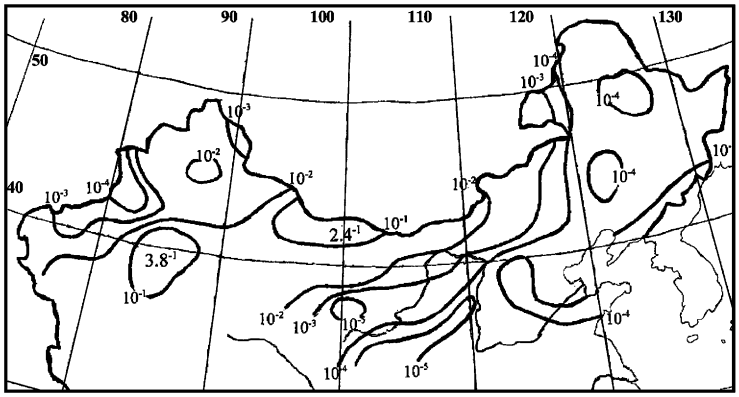

Fig. 6. Dust PM_{10} annual mean emission rates (ton/ha yr).

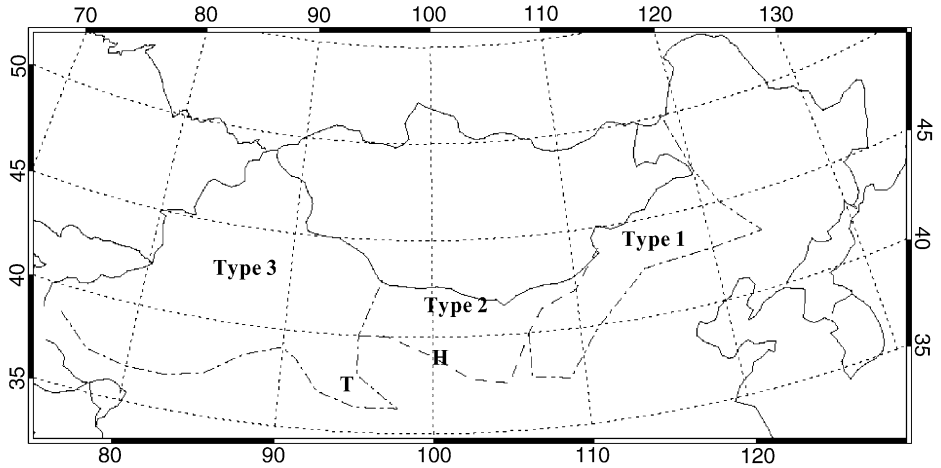

Fig. 7. Three types of dust sources: T—Tsaidam basin; H—Hexi Corridor.

Fig. 6 shows the PM_{10} dust annual mean emission rate, Q_{10}, calculated following the framework described in Section 2. PM_{10} dust emission rates in Northern China increase from east to west by five orders of magnitude. The contours of the emission rates higher than 10^{-1} ton/ha yr define two strongest dust source regions: one is in the Taklimakan Desert and the other is in the west part of the Inner-Mongolia Plateau. The PM_{30} and PM_{50} dust emissions show similar spatial distributions.

3.2. Comparative characterization of dust sources in Northern China

The above discussion reveals that Northern China is a complex, inhomogeneous dust production region comprising various types of individual sources of distinct properties and different strengths. Based on the integrated set of the factors introduced above, we identified the following three broad types of dust sources in Northern China (see Fig. 7): Type 1. Deserts in dry-agricultural areas; Type 2. Gobi-deserts and deserts located on the plateaus; and Type 3. Deserts and gobi-deserts located in topographical lows. Type 3 sources agree well with the suggestion by Prospero et al. (2002) that prodigious dust sources should be located in the basins or flanks of mountains. However, our Types 1 and 2 sources do not obey this rule. In turn, Type 2 sources agree with the study by Sun et al. (2001) and work of many Chinese and Japanese meteorologists (e.g., CEA, 2001; Nagoya University, 1995) who suggested that the Central gobi-desert and the deserts on the Alxa Plateau (Type 2 sources) are the main dust sources in China.

Type 1 sources consist of the Hulun Buir, Horqin, Hunshandake, Mu Us and Hobq Deserts, Type 2 sources include the Central gobi-desert, Ulan Buh Desert, Tengger Desert, Badain Jaran Desert and the

gobi-deserts in the Hexi Corridor, and Type 3 sources mainly comprises the Taklimakan, Gurbantunggut and Kumtag Deserts, Hashun gobi-desert, Turpan-Hami Basin (gobi-desert) and Tsaidam Basin (gobi-desert and playa). Type 3 sources are located in the basins or on flanks of high mountains, while Types 1 and 2 sources are located on the Inner-Mongolia Plateau and Alxa Plateau (elevation of 1000–1800 m), except for the Horqin Desert located on the Manchurian Plain (elevation of 400 m) and the Hexi Corridor (elevation of 800–1200 m). The Hexi Corridor is a low and narrow valley between high mountains, stretching roughly from east to west for about 1000 km.

3.2.1. Commonalities and specific features of individual dust sources

Types 1–3 sources, stretching from about east to west across Northern China, have specific differences associated with the east-to-west gradual changes of the main climatic, geographical, and pedological characteristics. Comparative characterization of dust sources is given in Table 2.

From east-to-west, the precipitation decreases from 400 to 20 mm/yr and aridity increases from 2 to 70 resulting in the surface type changes ranging from the farmlands, dry-grasslands to extremely arid regions such as the Taklimakan Desert. Type 1 sources and the east part of the Hexi Corridor (Type 2 source) are located in the dry-agricultural area. The name "dry-agricultural" means that farming strongly depends on irrigation, though a large population lives in this region. In contrast, most of Types 2 and 3 sources lie in the extreme arid areas where people can live only in small oases.

Exhaustive farming, over-grazing and improper use of the limited water resources have resulted in a severe desertification in Northern China. In particular, the desertification has speeded-up after 1950s under the pressure of rapidly growing population (CEA, 1998). Statistical analysis shows that the desert areas in Northern China were increased on average 1560 km^2/yr from 1950s to 1970s, 2100 km^2 in the 1980s and 2460 km^2 in the 1990s (Zhu and Zhu, 1999). Desertification affected all three types of dust sources. For instance, the Hulun Buir and Horqin deserts (Type 1 sources) were formed recently in the 20th century (Zhu and Zhu, 1999; CEA, 1998; Huasheng Daily, 2001). Using data from Zhang et al.(1998), we estimated that human activities have converted about 4.2×10^4 km^2 of grasslands into deserts in Type 2 sources and 1.84×10^4 km^2 of oases into deserts in Type 3.

Diverse topography of Northern China results in a complex pattern of wind fields. The strongest winds, associated with cold fronts, are observed on the high Inner-Mongolia Plateau (Type 2 sources). The annual mean wind speed in Type 2 sources is in the range from 3 to 5 m/s, while in the spring and winter the wind speed is usually higher on about 1 m/s than the annual mean. In contrast, the Taklimakan Desert (Type 3 source), lying in the basin, has lower annul mean wind speeds of 2–4 m/s.

East-to-west variations of precipitation and aridity also affect the distribution of soil types, soil composition, and soil texture in Northern China. Although the soil texture has a complex spatial distribution, there is a general tendency of a decrease of coarse particles and an increase of fine particles in surface soils from west-to-east: soil texture changes from gravelly sand soil, sand soil, loam to clay soil (Xiong, 1986). This tendency is governed by the weathering processes ranging from the dominant physical weathering in the west to the chemical weatherizing in the east due to the strong west-to-east gradient in precipitation.

According to our calculations, 8.4 million tons of PM_{10} dust are emitted annually into the atmosphere from the source region of some 1.99×10^6 km^2 in Northern China. The contributions of Types 1–3 sources to the total annual mean PM_{10} dust emission are 1%, 35% and 64%, respectively.

3.2.2. Spatial and temporal variability of dust emission

The strength of dust sources greatly increases from east-to-west across Northern China reflecting gradual changes in precipitation and aridity. The PM_{10} dust emission rate increases from east-to-west by as much as five orders of magnitude (Fig. 6). PM_{30} and PM_{50} dust emissions show a similar spatial distribution (Xuan, 1999; Xuan et al., 2000).

The most severe dust storms all occur in the spring season (Xu and Hu, 1996) when the surface is the driest and winds are the strongest (Table 2). This suggests that the high aridity and strong winds are two key elements governing the dust emission in Northern China. This conclusion is further supported by our analysis of the seasonal patterns of dust emission in three source types.

To estimate the seasonal variability, we partitioned the annul mean emission rate Q_{10} into the seasonal means, Q_1, Q_2, Q_3 and Q_4, according to the seasonal values of the climatic factor, $C = 0.504\,u^3/\mathrm{PE}^2$. The seasonal mean wind speed and seasonal Thornthwaite's index were used to perform these calculations.

Table 2 shows the seasonal mean dust emission in three source types. All three source types show the largest emission in the spring, while the lowest dust emission occurs in the summer season. From the data listed in Table 2, one can relate the spring emission maximum to the highest winds and highest aridity occurred in each source type. In turn, both aridity and winds are lowest in summer.

Along with the similarities, several noticeable differences in the seasonal cycle of the dust emission in three source types can be pointed out. Type 1 sources have

Table 2
Comparative characterization of three types of dust sources

Characteristics	Type 1	Type 2	Type 3
Topography[a,b]	Plateau, elevation of 500–1800 m, except the Horqin Desert	Plateau, elevation of 1000–1800 m, except the Hexi Corridor	Basin or mountain flank, elevation of 300–1200 m, except the Tsaidam Basin
Surface type[c]	Farmland: 6.82×10^4 km^2 Grassland: 58.11×10^4 km^2 Desert: 13.76×10^4 km^2	Farmland: 3.05×10^4 km^2 Grassland: 31.65×10^4 km^2 Desert and gobi-desert: 26.53×10^4 km^2	Farmland: 1.81×10^4 km^2 Grassland: 44.36×10^4 km^2 Desert and gobi-desert: 59.08×10^4 km^2
Population[c]	11.3×10^6	14.6×10^6	9.6×10^6
Frequency of dust storm occurrence	High-frequency area	Extra-high frequency area	High and extra-high frequency areas
Surface soil texture (%)[e]	Gravel: 0; Sand: 46; Loam: 51; Clay: 0	Gravel: 7; Sand: 62; Loam: 31; Clay: 0	Gravel: 5; Sand: 65; Loam: 30; Clay: 0
Surface soil composition[d,e]			
Main minerals	Quartz, carbonates	Quartz, gypsum, carbonates, chlorides	Quartz, gypsum, chlorides, carbonates
Chemical composition (%)	Si: ~25[f], Al: 3–7.5, Ca: 1–3, Fe: 1–3, K: 1.6–2.7, Na: 0.5–1.8, Mg: 0.4–1, Ti: 0.1–0.4	Si: ~32[f], Al: 3–7.5, Ca: 2–6, Fe: 1–3.5, K: 1.2–2.4, Na: 0.5–2.2, Mg: 0.6–1.4, Ti: 0.1–0.4	Si: ~ 31[f], Ca: 3–8, Al: 3–7.5, Fe: 1.5–3.5, K: 0.8–2.4, Mg: 1.0–2.0, Na: 0.5–2.2, Ti: 0.2–0.4
Mean wind speed (m/s)[g]			
Annual	2–4	3–5	2–4
Spring	3–6	3–6	2–6
Summer	2–4	3–5	2–5
Fall	3–4	2–5	2–4
Winter	2–5	3–6	1–4
Mean precipitation (mm)[g]			
Annual	200–400	50–200	20–100
Spring	30–50	10–30	5–30
Summer	100–300	30–100	20–50
Fall	50–75	10–50	1–20
Winter	5–10	1–5	1–10
Mean aridity[h]			
Annul	2–4	4–40[i]	10–70[i]
April	5–10	10–100	10–200
July	1–2	2–10	10–50
October	2–5	5–50	5–200
January	1–10	5–50	5–50

Table 2 (*continued*)

Characteristics	Type 1	Type 2	Type 3
Mean dust emission (ton)			
Annual	$Q_{10} = 0.092 \times 10^6$	$Q_{10} = 2.9 \times 10^6$	$Q_{10} = 5.4 \times 10^6$
	$Q_{30} = 0.2 \times 10^6$	$Q_{30} = 6.9 \times 10^6$	$Q_{30} = 17.6 \times 10^6$
	$Q_{50} = 0.5 \times 10^6$	$Q_{50} = 13.2 \times 10^6$	$Q_{50} = 28.9 \times 10^6$
Spring	$Q_{10} = 0.07 \times 10^6$	$Q_{10} = 1.5 \times 10^6$	$Q_{10} = 3.4 \times 10^6$
Summer	$Q_{10} = 0.002 \times 10^6$	$Q_{10} = 0.3 \times 10^6$	$Q_{10} = 0.2 \times 10^6$
Fall	$Q_{10} = 0.01 \times 10^6$	$Q_{10} = 0.3 \times 10^6$	$Q_{10} = 1.5 \times 10^6$
Winter	$Q_{10} = 0.01 \times 10^6$	$Q_{10} = 0.8 \times 10^6$	$Q_{10} = 0.3 \times 10^6$

[a] Zhu and Zhu (1999).
[b] CEA (1998).
[c] Zhang et al. (1998).
[d] Zheng (1994).
[e] Xiong (1986).
[f] Nagoya University (1995).
[g] Zhao (1994).
[h] Lao (1999).
[i] Upper-limits are from Zhang et al. (1998).

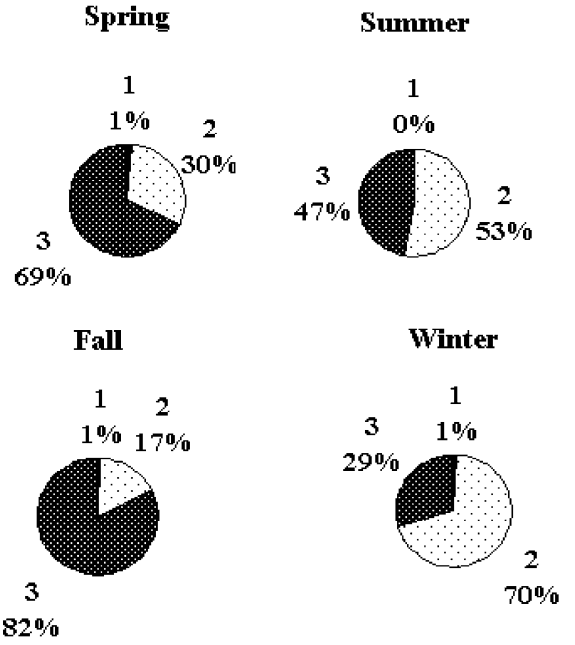

Fig. 8. Relative contribution of three types of sources to the total dust emission in Northern China.

one spring peak and much lower dust amount is emitted in the other seasons, though winter and fall dust emission is about the same (see Table 2). This seasonal cycle agrees well with the study by Littmann (1991) based on the analysis of dust storm frequency recorded at the Taiyuan weather station located in this source region. In contrast, Type 2 sources emit more PM_{10} dust in winter than in fall. This can be explained by very strong winds observed in winter (3–6 m/s, same as in spring) and relatively high aridity of about 5–50 (half of the value on the spring season). In turn, Type 3 sources show a second peak in the fall in agreement with dust storm records at the Urumqi weather station (Littmann, 1991). We explain this second peak by extreme aridity observed in fall in this source region—aridity in fall is as high as in spring (about 5–200). One can conclude that the second highest value of the dust emission in Type 2 sources is caused by both high winds and high aridity in winter, while the second peak value of Type 3 sources is mainly due to extreme aridity in fall.

Fig 8 shows the relative contribution of each source type to the total seasonal dust emission in Northern China. Type 3 sources dominate the dust emission in the spring season, as well as in the annual mean. On the other hand, Type 2 sources emit more dust than in winter because of the cold waves passing the Mongolian Plateau. Type 1 sources are relatively weak, contributing some 1% to total PM_{10} dust emission during all four seasons.

3.2.3. Dust emission in the Loess Plateau and gobi-deserts

The Loess Plateau lies in the dry-agricultural area to the south of the Type 1 source region. It seems to be a potential dust emission source because its surface soil consists of fine silt and clay particulates. Several studies considered the Loess Plateau as a major dust source in China (e.g., Chun et al., 2001). However, observations revealed the low frequency of dust storm occurrences in this region, except in its northwest part adjacent to deserts (see Fig. 5). Our calculations of dust emission rates also suggest that the vast area of the Loess Plateau is not a strong dust source compared to other regions (Fig. 6). The possible explanation is in the high clay content. Some studies suggested that water erosion is the main problem on Loess Plateau rather than wind erosion (Zhang, 1991).

The ability of the gobi-deserts in Northern China to emit dust into the air is not only interesting but also, sometimes, confusing. Both the dust storm frequency (Fig. 5) and dust emission rate (Fig. 6) demonstrate that the Central gobi-desert and Hashun gobi-desert, alternatively covered by gravel, sands and soils (Xiong, 1986), are a prodigious dust source. The ability of the gobi desert to emit dust is also supported by the measurements which show that the gravel buried in sand (soil) surfaces can promote the dust emission (Gillette, 1983). Thus, we suggest that the Central gobi-desert is the second largest source of dust in Northern China after the Taklimakan Desert.

A large part of the Central gobi-desert, including Altajn Caadah gobi-desert, Borzongijn gobi-desert and Albyn gobi-desert, lies in the Republic of Mongolia. It covers the area of about $2.6 \times 10^5\,km^2$ (MacMillan, 1992). Taking the dust emission rate calculated for Central gobi-desert, we estimate that the Mongolian part of the Central gobi-desert emits annually 4.7×10^6, 10.5×10^6 and 20.1×10^6 tons of PM_{10} PM_{30}, PM_{50} dust, respectively.

3.3. Dust emission in the Hexi Corridor and Tsaidam Basin

Historically, the Hexi Corridor, the east part of the famous 'Silk Road', has been a link between ancient east and west cultures. It is a narrow valley surrounded by high mountains on both sides. As a dust source, it combines some features of Types 1–3 sources. From east to west along the Hexi Corridor, annual precipitation decreases from 200 to 50 mm/yr (Zhao, 1994), while the aridity increases from 4 to 16 (Zhang et al., 1998). As a result, the east part of the Hexi Corridor lies in a dry-agricultural area (Type 1 sources), while there are many deserts and different kinds of gobi-deserts in its west part (Type 2 sources). The Hexi Corridor also has some features of Type 3 sources since it is located in the topographical low. The frequency of dust storms in the Hexi Corridor is very high ranging from 63 to 128 d/yr (Zhang et al., 1998).

The Tsaidam Basin (area of $2.5 \times 10^4\,km^2$ and elevation of 2600–3400 m) is located in the north part of the Qinghai-Tibetan Plateau. It is a dry and cold alpine basin, consisting of deserts, gobi-deserts, oases, and playas. The annual mean wind speed is about 3–4 m/s and annual mean precipitation is less than 30 mm/yr. The Tsaidam basin belongs to the high frequency area of dust storms with more than 20 days per year (Fig. 5). Because the basin lies in the cold alpine area, its ground surface remains frozen until the late spring. The solid frozen crust prevents the dust emission even when winds are strong. Therefore, the Tsaidam Basin is an active dust source only in late spring and early summer (Ma, 1997). It is likely that dust sources on the even higher Tibetan Plateau have the similar seasonal dust emission pattern. Currently, we included the Tsaidam Basin into the Type 3 sources, though the above discussion indicates that the sub-types of each broad type of dust sources would be required in further analysis.

4. Summary

Northern China is one of the main sources of atmospheric mineral dust. To characterize the individual source regions, we have been compiling the Asian Dust Databank, which currently comprises the geographical, pedological and 30 yr (1951–1980) climatological data from 301 meteorological stations in Northern China. This databank in conjunction with the modified US EPA empirical formulas for dust emission rates enabled us to perform comprehensive characterization of dust sources and to estimate their strengths on the climatic (30 yr mean) time scale. Our main findings are the following:

(1) We identified three broad types of dust sources in Northern China: Type 1. Deserts in dry-agricultural areas; Type 2. Gobi-deserts and deserts located on the plateaus; and Type 3. Deserts and gobi-deserts located in topographical lows.
(2) Our analysis confirmed that the Taklimakan Desert (Type 3 source) is a main source of atmospheric dust in Northern China. The next important sources are the Central gobi-desert and the deserts on the Alxa Plateau. The Loess Plateau appears to be a weak dust source. Although Types 1 and 2 sources are not located in the basins as the Taklimakan Desert, they are a prodigious dust source because of high aridity and strong winds.
(3) The annual mean dust emission of PM_{50}, PM_{30} and PM_{10} is 42.6, 24.8 and 8.4 million tons, respectively.

Of these, more than half of the total annual dust is emitted in the spring season. Relative contributions of Types 1–3 sources to annul mean PM_{10} dust emission is about 1%, 35% and 64%, respectively.

(4) Analysis of both the spatial distribution and seasonal variation pattern of dust emission revealed that each source type has a distinct seasonal cycle, though the maximum of dust production occurs in the spring. Seasonal cycles can be explained by the specific seasonal variation of wind speed and aridity in each source type.

(5) The strength of dust sources greatly increases from east-to-west across Northern China reflecting gradual changes in precipitation and aridity.

(6) Human activities, mainly exhaustive farming, overgrazing and improper use of limited water resources in arid and semi-arid lands, have been seriously damaging the natural environment in Northern China, likely causing the expansion of dust sources and increase of their dust emission strength.

Our findings have several important implications. Mineral dust frequently dominates the aerosol mass over the Central Asia and the Pacific Ocean. Therefore, the climatological seasonal variation of dust emissions might modulate the aerosol radiative forcing of climate, as well as atmospheric chemistry and acidification of precipitation over the large regions. In addition, it can affect the amount of mineral dust deposited to the oceans and hence the main biochemical cycles (Gao et al., 2001).

Further progress in understanding the diverse impacts of Asian dust would require the integrated analysis of inter-annual variability of dust mobilization and transport, as well as an improved dust emission scheme. It would be important to relate the dust emission in three types of dust sources to the preferential transport routes of dust outbreaks suggested by several previous studies (e.g., Chen and Chen, 1987; Sun et al., 2001), though the additional analysis of meteorological conditions in conjunction with satellite data would be required.

Acknowledgements

This study was supported by the National Science Foundation grant ATM-0002746. The authors are grateful to Mr. Guoliang Liu and Mr. Ke Du for their help with dust emission calculations.

References

Bagnold, R.A., 1941. The Physics of Blown Sand and Desert Dunes. Methuen, London.

CEA (China Environmental Administration), 1998. Study on Combating Desertification: Land Degradation in China. China Environmental Science Press, Beijing, pp. 6–9,11–20.

CEA (China Environmental Administration), 2001. Integrated Investigation Team of Sandstorms: More sandstorms in oncoming years. China News Service (web site), April 14.

Chao, S., 1984. The sandy deserts and the gobi of China. In: El-Baz (Ed.), Deserts and Arid Lands. Martinus Nijhoff Publishers, Boston, pp. 95–143.

Chen, G.T.-J., Chen, H.-J., 1987. Study on large-scale features of duststorm system in East Asia. Papers in Meteorological Research. The Meteorological Society of the Republic of China 10, 57–79.

Chun, Y., Boo, K., Kim, J., Park, S., Lee, M., 2001. Synopsis, transport, and physical characteristics of Asian dust in Korea. Journal of Geophysical Research 106, 18461–18469.

CMA (China Meteorological Administration), 1979. Weather Observatory Regulations. Meteorology Press, Beijing, pp. 16–20.

Cowherd, C., Bohn Jr., R., Cuscino, T., 1979. Iron and steel plant open source fugitive emission evaluation. EPA-600/2-79-103.

Draxler, R., Gillette, D.A., Kirkpatrick, J.S., Heller, J., 2001. Estimating PM_{10} air concentrations from dust storms in Iraq, Kuwait, and Saudi Arabia. Atmospheric Environment 35, 4315–4330.

Duce, R.A., 1995. Sources, distributions, and fluxes of mineral aerosols and their relationship to climate. In: Charlson, R.J., Heintzenberg, J. (Eds.), Aerosol Forcing of Climate. Wiley, New York, pp. 43–72.

Gao, Y., Kaufman, Y.J., Tanre, D., Kolber, D., Falkowski, P.G., 2001. Seasonal distribution of aeolian iron fluxes to the global ocean. Geophysical Research Letters 28, 29–32.

Gillette, D., 1979. Environmental factors affecting dust emission by wind erosion. In: Morales, C. (Ed.), Saharan Dust. Wiley, New York, pp. 71–94.

Gillette, D., 1983. Threshold velocities for wind erosion on natural terrestrial arid surfaces. In: Pruppacher, H., et al. (Ed.), Precipitation Scavenging, Dry Deposition and Resuspension. Elsevier, New York.

Goudie, A.S., Middleton, N.J., 1992. The changing frequency of dust storms through time. Climatic Change 20, 197–225.

Greeley, R., Iversen, J.D., 1985. Wind as a Geological Process on Earth, Mars, Venus and Titan. Cambridge University Press, New York, 333pp.

Hao, J., Guo, F., Xuan, J., 1996. Statistics and analysis of aeolian sand-dust phenomenon in Beijing area. Proceedings of the Second International Joint Seminar on the Regional Deposition Processes in the Atmosphere, Beijing, China, October, p.114.

Huang, Z., 1997. Historical records of dust storms in northwest China. In: Fang, Z., et al. (Ed.), Studies of China dust Storms. Meteorology Press, Beijing, pp. 31–36.

Huasheng Daily, 2001. Sand storm from Horqin Desert. Huasheng Daily (web site), April 25, 2001.

IPCC, Climate Change, 2001. The scientific basis. In: Houghton, J.T., et al. (Eds.), Contribution of Working Group I to the Third Assessment Report of the Intergovernmental Panel on Climate Change. University Press, Cambridge, United Kingdom and New York, NY, USA, 881pp.

Lao, K. (Ed.), 1999. National Physical Atlas of China. Cartographic Publishing House, Beijing.

Littmann, T., 1991. Dust storm frequency in Asia: climatic control and variability. International Journal of Climatology 11, 393–412.

Liu, M., Westphal, D.L., 2001. A study of the sensitivity of simulated mineral dust production to model resolution. Journal of Geophysical Research 106, 18331–18344.

Ma, Y., 1997. Case study of the dust storm of 28 April 1992 in Qinghai. In: Fang, Z., et al. (Ed.), Studies of China Dust storms. Meteorology Press, Beijing, pp. 59–61.

MacMillan, 1992. The Book of the World. MacMillan, USA.

Marticorena, B., Bergametti, G., 1995. Modeling the atmospheric dust cycle: 1. Design of a soil-derived dust emission scheme. Journal of Geophysical Research 100, 16415–16430.

Marticorena, B., Bergametti, G., Aumont, B., 1997. Modeling the atmospheric dust cycle: 2. Simulation of Saharan dust sources. Journal of Geophysical Research 102, 4387–4404.

Nagoya University, 1995. Yellow Sands (Chinese Version). China Construction Press, Beijing, pp. 85–99.

OAQPS (EPA), 1977. Guideline for development of control strategies in areas with fugitive dust problems. EPA-405/2-77-029.

Prospero, J., Ginoux, P., Torres, O., Nicholson, S., 2002. Environmental characterization of global sources of atmospheric soil dust derived from the NIMBUS-7 TOMS absorbing aerosol product. Reviews of Geophysics, in press.

Qian, Z., He, H., Qu, Z., Chen, M., 1997. Classification, case analyses and statistical characters of dust storms in northwest China. In: Fang, Z., et al. (Ed.), Studies of China Dust Storms. Meteorology Press, Beijing, pp. 1–10.

Sokolik, I.N., Winker, D., Bergametti, G., Gillette, D., Carmichael, G., Kaufman, Y., Gomes, L., Schuetz, L., Penner, J., 2001. Introduction to special section on mineral dust: outstanding problems in quantifying the radiative impact of mineral dust. Journal of Geophysical Research 106, 18015–18028.

Sun, J., Zhang, M., Liu, T., 2001. Spatial and temporal characteristics of dust storms in China and its surrounding regions, 1960–1999: relations to source area and climate. Journal of Geophysical Research 106, 10325–10333.

Tegen, I., Fung, I., 1995. Contribution to the atmospheric mineral aerosol load from land source modification. Journal of Geophysical Research 100, 18707–18726.

Tegen, I., Miller, R., 1997. Contribution of different aerosol species to the global aerosol extinction optical thickness; estimates from model results. Journal of Geophysical Research 102, 23895–23915.

Uno, I., Amano, H., Emori, S., Kinoshita, N., Matsu, I., Sugimoto, N., 2001. Trans-Pacific yellow sand transport observed in April 1998: a numerical simulation. Journal of Geophysical Research 106, 18331–18344.

Westphal, D.L., Hogan, T.F., Liu, M., 1998. Dynamical forcing of the Chinese dust storms of April 1998. In: Presented at the Fall Meeting of the American Geophysical Union, San Francisco, 9–13 December, 1998.

Xiong, Y. (Ed.), 1986. Soil Atlas of China. Cartographic Publishing House, Beijing, pp. 19–20, 23–24, 25–26.

Xiong, Y., Li, Q., 1990. Soil of China. Science Press, Beijing.

Xu, D., 1984. Wind characters of atmospheric boundary layer and its applications. Journal of Aerodynamics 3, 75–87.

Xu, Q., Hu, J., 1996. Spatial distribution and seasonal variation of dust storms in northwest China. Quarterly Journal of Applied Meteorology 7, 479–482.

Xuan, J., 1999. Dust emission factors for environment of Northern China. Atmospheric Environment 33, 1767–1776.

Xuan, J., Liu, G., Du, K., 2000. Dust emission inventory in Northern China. Atmospheric Environment 34, 4565–4570.

Zhang, T. (Ed.), 1991. Loess Plateau. Science Press, Beijing, pp. 14–22.

Zhang, J., Lin, Z., 1992. Climate of China. Wiley, New York, pp. 376.

Zhang, Q., Zhao, X., Zhao, H., 1998. Grasslands in Desert Area of China. Meteorology Press, Beijing, pp. 1–10.

Zhao, G. (Ed.), 1994. Atlas of Climate Resources of China. Cartographic Publishing House, Beijing.

Zhao, S., 1985. Physical Geography of China Arid Lands. Science Press, Beijing, pp. 1–17.

Zhao, X., 1997. Northwest China is the region of frequent dust storms. In: Fang, Z., et al. (Ed.), Studies of China Dust Storms. Meteorology Press, Beijing, pp. 27–30.

Zheng, C. (Ed.), 1994. Atlas of Soil Environmental Background Value in the People's Republic of China. China Environmental Science Press, Beijing.

Zhu, Z., Zhu, Zh., 1999. Combating Sandy Desertification in China. China Forestry Press, Beijing, pp.21–28, 62–67, 79–82.